DOI: 10.1021/ic9013637

Inorganic Chemistry
Article

Electronic Structure of the A_8Tr_{11} (A = K, Rb, Cs; Tr = Ga, In, Tl) Zintl Phases: Possible Chemical Reasons Behind Their Activated versus Non Activated Conductivity

Manuel Cobián,[‡] Pere Alemany,*[,†] Alberto García,[‡] and Enric Canadell*[,‡]

[†]*Departament de Química Física and Institut de Química Teòrica i Computacional* (*IQTCUB*), *Universitat de Barcelona, Diagonal 647, 08028 Barcelona, Spain, and* [‡]*Institut de Ciència de Materials de Barcelona* (*CSIC*), *Campus de la UAB, 08193 Bellaterra, Spain*

Received July 13, 2009

The electronic structure of the A_8Tr_{11} (A=K, Cs; Tr=Ga, In, Tl) Zintl phases has been studied by means of first-principles density functional theory (DFT) calculations. It is shown that the hypoelectronic Tr_{11} cluster in these phases must be considered as Tr_{11}^{8-} even if it would require just a 7− charge to maximize its bonding, filling all its bonding and nonbonding levels. Our calculations show that the lowest empty orbital of the isolated Tr_{11}^{7-} clusters is an a_1-type orbital. However, a degenerate e-type set of orbitals is higher but quite close in the case of the Ga_{11}^{7-} clusters. Thus, for the isolated Tr_{11}^{8-} clusters, the extra electron occupies always an a_1-type antibonding orbital that contains, however, some Tr−Tr bonding component thus leading to a weak global antibonding character. In the solid, cluster−alkali-metal bonding interactions occur and spread the cluster levels into bands, but the extra electron still fills the a_1-type cluster level for most of the A_8Tr_{11} phases. The cluster−alkali-metal interactions have a minor role in stabilizing this orbital but they provide the necessary delocalization to lead to the metallic character of these phases. In contrast, the e-type antibonding levels of the Ga_{11}^{7-} isolated cluster are those which become filled by the extra electron in the Cs_8Ga_{11} solid. This phase should be metallic, but occupation of this degenerate pair of cluster levels would lead to a structural instability that may be avoided by reducing the interactions of the alkali-metal atoms with the cluster levels. In that way the occupation appropriate for the isolated cluster is restored (i.e., one electron fills the a_1 cluster orbital), but the extra electron now remains localized on the cluster, thus leading to the unexpected activated conductivity observed for the Cs_8Ga_{11} phase.

Introduction

The relationship between the structure and the number of electrons in many intermetallic Zintl phases containing anionic clusters has been traditionally rationalized on the basis of Wade's rules.[1] This approach works very successfully as long as the clusters are deltahedral. The preparation of K_8In_{11},[2,3] containing In_{11} clusters, provided not only the first homoatomic indium cluster but also an example of a cluster that is stable for a number of skeletal electrons lower than that predicted by Wade's rules. In this phase, potassium cations are located between In_{11} clusters in such a way that every cluster is surrounded by 24 potassium cations (see Figure 1). Sevov and Corbett[2] showed that the low electron count was related to the strongly distorted geometry of the In_{11} cluster. In fact, this cluster is not at all deltahedral but can be described as a pentacapped trigonal prism where the triangular ends of the prism are considerably expanded. On the basis of extended Hückel calculations, these authors[2] showed that all the bonding levels of such a cluster are filled for an electron count corresponding to In_{11}^{7-} so that they proposed that this phase should be formally described as $(K^+)_8In_{11}^{7-}(e^-)$, with one electron mostly delocalized over the cations.[2] Cs_8Tl_{11},[4] Rb_8Tl_{11},[4,5] K_8Tl_{11},[4,6] Rb_8In_{11}[7] (although different attempts failed at reproducing this phase),[8] and Cs_8Ga_{11}[8] have also been reported, and all of them have the same structure except for small distortions of the Tr_{11} clusters which in some cases have D_{3h} symmetry but in others only D_3. In apparent agreement with the above-mentioned chemical description, most of these phases have been found to be metallic but, surprisingly, Cs_8Ga_{11} was

*To whom correspondence should be addressed. E-mail: p.alemany@ub.edu (P.A.), canadell@icmab.es (E.C.). Phone: +34 93 402 1239 (P.A.), +34 93 580 1853 (E.C.). Fax: +34 93 402 1231 (P.A.), +34 93 580 5729 (E.C.).

(1) (a) Corbett, J. D. *Inorg. Chem.* **2000**, *39*, 5178. (b) Corbett, J. D. *Angew. Chem., Int. Ed.* **2000**, *39*, 670. (c) Corbett, J. D. *Structr. Bonding* **1997**, *87*, 103. (d) *Chemistry, Structure and Bonding of Zintl Phases and Ions*; Kauzlarich, S., Ed.; VCH Publishers: New York, 1996, and references therein.
(2) Sevov, S. C.; Corbett, J. D. *Inorg. Chem.* **1991**, *30*, 4875.
(3) Blasé, W.; Cordier, G. *Z. Kristallogr.* **1991**, *194*, 150.
(4) Dong, Z.-C.; Corbett, J. D. *J. Cluster Sci.* **1995**, *6*, 187.
(5) Cordier, G.; Müller, V. *Z. Kristallogr.* **1993**, *203*, 152.
(6) Cordier, G.; Müller, V. *Z. Kristallogr.* **1992**, *198*, 281.
(7) Cordier, G.; Müller, V. *Z. Kristallogr.* **1993**, *203*, 154.
(8) Henning, R. W.; Corbett, J. D. *Inorg. Chem.* **1997**, *36*, 6045.

Published on Web 09/10/2009

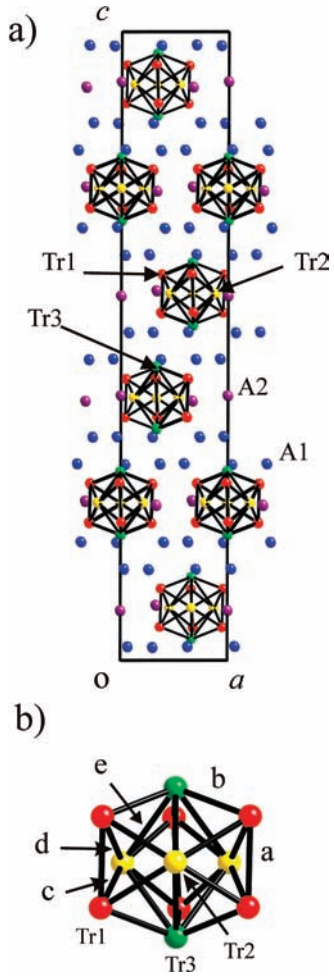

Figure 1. A_8Tr_{11} phases: (a) crystal structure ($R\bar{3}c$) and (b) Tr_{11} clusters, showing the atom and cluster bond labeling used in the present work.

found to behave as a semiconductor.[8] It is worthwhile noting that several halide phases like $Cs_8Ga_{11}Cl$, $Rb_8Ga_{11}Cl$, $Cs_8Tl_{11}Br$, and so forth have also been prepared.[8] The A and Tr positions in these phases are essentially the same as those in the corresponding binary compounds, and the halogen fills voids within the alkali-metals' sublattice. $Cs_8Ga_{11}Cl$ is a diamagnetic semiconductor, something which is consistent with the $(Cs^+)_8Ga_{11}{}^{7-}(Cl^-)$ formulation for this phase.[8] Isolated $Tl_{11}{}^{7-}$ clusters are also present in the structurally more complex ternary phase $K_{14}Cd_9Tl_{21}$,[9] and palladium centered Tl_{11} clusters have been found in $A_8Tl_{11}Pd_x$ (A = Cs, Rb, K; $x = 0.84-0.68$).[10]

Despite the structural similarity of the A_8Tr_{11} phases, Cs_8Ga_{11} exhibits a clearly different physical behavior. Whereas all other phases exhibit Pauli paramagnetism, Cs_8Ga_{11} is paramagnetic and follows a Curie−Weiss law above 90 K, when some kind of structural transition occurs accompanied (or followed) by a magnetic transition.[8] However, it has not been possible to obtain structural data at low temperatures. Thus, the magnetic susceptibility studies suggest that the extra electron must be localized in Cs_8Ga_{11} but delocalized in the other A_8Tr_{11} phases. This is confirmed by the resistivity measurements, since Cs_8Ga_{11} exhibits activated conductivity whereas the other A_8Tr_{11} phases are metals.[8] This is a puzzling result. Whereas one may feel comfortable with the idea that the extra electron, which is not needed to fulfill the electronic requirements for the cluster stability, is actually delocalized along the cationic sublattice of these salts, it is difficult to understand how this extra electron may localize in Cs_8Ga_{11} if it is not on the cluster. However, according to the extended Hückel studies, such electron would fill a high-lying antibonding orbital which, in addition, is doubly degenerate (e). Consequently, in contrast with the experimental results, a Jahn−Teller distortion lowering the D_3 symmetry of the cluster would be expected. All these observations show that there is a clear need for a detailed electronic structure study of these phases which can provide grounds on which to discuss the two following questions: where is the extra electron? and what makes Cs_8Ga_{11} different from the other presently known A_8Tr_{11} phases?

To the best of our knowledge the electronic structure of K_8In_{11} has been the object of two previous studies. Blasé et al.[11] carried out extended Hückel calculations which confirmed that the clusters should be described as $In_{11}{}^{7-}$ and the extra electron should fill potassium−indium bonding levels. However, recent work on Zintl phases like K_5Bi_4,[12a] K_3Bi_2,[12b] $Ba_7Ga_4Sb_9$,[12c] Li_2Ga,[12d] and so forth has clearly shown that a meaningful discussion of aspects related to the actual degree of charge transfer in Zintl-type phases must be based on accurate first-principles calculations. Both the neglect of Coulomb interactions and the uncertainty in the relative values of the parameters for the alkali and non-alkali metals used in extended Hückel calculations may seriously affect the degree of mixing of their orbitals, a central issue here. Llusar et al.[13] carried out periodic Hartree−Fock calculations and proposed on the basis of an analysis of the integrated density that the extra electron is delocalized over the potassium layers. However, the density of states (DOS) plots reported by these authors strongly suggest that the electrons underlying the metallic character of the system are mostly associated with the indium clusters. Thus, none of these studies seem to provide an adequate answer to the two previous questions. Here we report a first-principles study of the electronic structure of several of these phases which we believe offers a plausible explanation of the origin of their different physical behavior.

Computational Details

First-principles calculations for Cs_8Ga_{11}, $Cs_8Ga_{11}Cl$, Cs_8Tl_{11} and K_8In_{11} were carried out using a numerical atomic orbitals DFT approach,[14] developed for efficient calculations in large systems and implemented in the SIESTA code.[15−17]

(9) Tillard-Charbonnel, M.; Chahine, A.; Belin, C.; Rousseau, R.; Canadell, E. *Chem. Eur. J.* **1997**, *3*, 799.
(10) Kaskel, S.; Klem, M. T.; Corbett, J. D. *Inorg. Chem.* **2002**, *41*, 3457.
(11) Blasé, W.; Cordier, G.; Müller, V.; Häussermann, U.; Nesper, R.; Somer, M. *Z. Naturforsch.* **1993**, No. 48b, 754.
(12) (a) Rodríguez-Fortea, A.; Canadell, E. *Inorg. Chem.* **2003**, *42*, 2759. (b) Alemany, P.; Llunell, P.; Canadell, E. *Inorg. Chem.* **2005**, *44*, 1646. (c) Alemany, P.; Llunell, P.; Canadell, E. *Inorg. Chem.* **2006**, *45*, 7235. (d) Alemany, P.; Llunell, P.; Canadell, E. *Inorg. Chem.* **2005**, *44*, 374.
(13) Llusar, R.; Beltrán, A.; Andrés, J.; Silvi, B.; Savin, A. *J. Phys. Chem.* **1995**, *99*, 12483.
(14) (a) Hohenberg, P.; Kohn, W. *Phys. Rev.* **1964**, *136*, B864. (b) Kohn, W.; Sham, L. J. *Phys. Rev.* **1965**, *140*, A1133.
(15) Soler, J. M.; Artacho, E.; Gale, J. D.; García, A.; Junquera, J.; Ordejón, P.; Sánchez-Portal, D. *J. Phys.: Condens. Matter* **2002**, *14*, 2745.
(16) http://www.uam.es/siesta/.
(17) For a review on applications of the SIESTA approach in materials science see: Sánchez-Portal, D.; Ordejón, P.; Canadell, E. *Struct. Bonding* **2004**, *113*, 103.

Table 1. Intra Cluster Bond Lengths (Å) for Cs_8Tl_{11}, K_8In_{11}, and Cs_8Ga_{11}[a]

bond	bonded atoms	number of bonds per cluster	Cs_8Tl_{11}	K_8In_{11}	Cs_8Ga_{11}
a	Tr1−Tr1	3	3.230	3.102	2.756
b	Tr1−Tr3	6	3.150	3.053	2.681
c	Tr1−Tr2	6	3.067	2.967	2.642
d	Tr1−Tr2	6	3.150	3.063	2.680
e	Tr2−Tr3	6	3.440	3.284	2.913

[a] See Figure 1b for the labeling.

We have used the generalized gradient approximation to DFT and, in particular, the functional of Perdew, Burke, and Ernzerhof.[18] Only the valence electrons are considered in the calculation, with the core being replaced by norm-conserving scalar relativistic pseudopotentials[19] factorized in the Kleinman−Bylander form.[20] The 3d electrons of Ga, 4d electrons of In, 5d electrons of Tl, 5p electrons of Cs and 3p electrons of K were treated as valence electrons. We have used an optimized[21,22] split-valence double-ζ basis set including polarization orbitals for all atoms. The energy cutoff of the real space integration mesh was 300 Ry, and the Brillouin zone was sampled using grids of $(9 \times 9 \times 9)$ k-points.[23] All calculations reported in this work have been carried out using the experimental rhombohedral cell.[2,4,8]

Results and Discussion

The rhombohedral crystal structure of the A_8Tr_{11} phases ($R\bar{3}c$) is shown in Figure 1a. It is built from isolated Tr_{11} clusters arranged in layers perpendicular to the c-direction. These clusters are separated by two types of crystallographically inequivalent alkali-metal atoms. The A1 atoms (in blue) form slabs separating the layers of the Tr_{11} clusters whereas the A2 atoms (in purple) fill the voids in the cluster layers. In this way, every Tr_{11} cluster is surrounded by 24 alkali-metal atoms (18 A1 and 6 A2). The Tr_{11} clusters (see Figure 1b for atom and bonds labeling) can be described as pentacapped trigonal prisms although the cluster is so compressed along the 3-fold axis that the six Tr−Tr distances within the triangles are too long to have any bonding significance. The loss of the six Tr1−Tr1 bonds is partially compensated by the development of six relatively long but non negligible Tr2−Tr3 bonds (noted "e" in Figure 1b). Thus, the Tr_{11} cluster (see Figure 1b) holds a series of three Tr1−Tr1 bonds ("a"), six Tr1−Tr3 bonds ("b"), twelve Tr2−Tr1 bonds ("c" and "d"), and six Tr2−Tr3 bonds ("e"). The experimental bond lengths for Cs_8Tl_{11}, Cs_8Ga_{11} and K_8In_{11} are reported in Table 1.

Shown in Figure 2 is the DOS as well as the cesium local DOS calculated for Cs_8Tl_{11} (recall that in DFT approaches using localized basis sets such as the present one, the total DOS is simply the addition of those of the different atomic contributions). The contribution of the thallium 5d orbitals which occurs at lower energies, around −12 eV, is not included in Figure 2. All contributions below −4 eV are

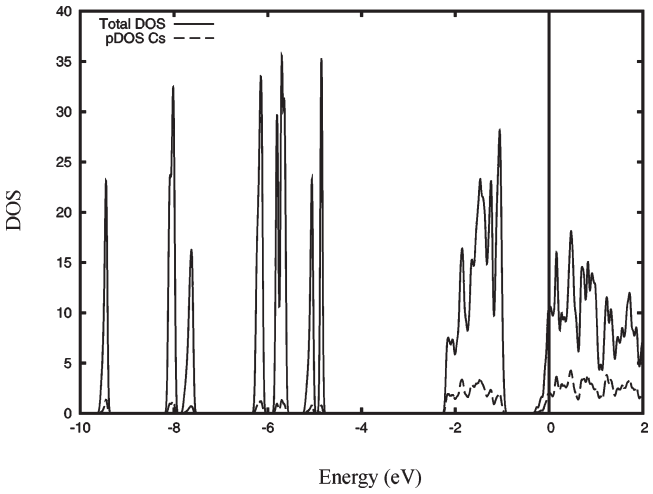

Figure 2. Calculated DOS for Cs_8Tl_{11} as well as the local contribution of the Cs atoms.

mostly thallium 6s in character with weak cesium contributions and account for 22 electrons per Cs_8Tl_{11} formula unit. The wide component centered around −1.5 eV is built from the thallium 6p orbitals but contains a very substantial contribution from the cesium levels. Integration of this contribution leads to a total of 18 electrons per Cs_8Tl_{11} formula unit. Consequently, since all levels below the energy gap around −0.4 eV are mostly cluster in character, if the Fermi level was in this gap, there would formally be a total of 40 electrons per cluster which thus should be described as Tl_{11}^{7-}. The results of Figure 2 are in complete agreement with the description of the electronic structure of the discrete Tr_{11} clusters given by Sevov and Corbett:[2] nine bonding levels accounting for $2n - 4$ (n being the number of vertices of the cluster) skeletal electrons of the cluster below which occur 11 s levels of the Tr atoms. The key feature of Figure 2 is, however, that the extra electron needed to reach the 41 electrons per formula unit is concentrated on the cluster: at the Fermi level, 81% of the DOS originates from the Tl_{11} clusters. This is also the case for the other A_8Tr_{11} phases we have studied: 67.2% for Cs_8Ga_{11} and 72.1% for K_8In_{11}. Thus we can quite firmly answer the first question raised in the introduction: *the extra electron mostly goes to an antibonding orbital of the cluster* which is somewhat stabilized through bonding interactions with the more higher-lying levels of the alkali-metal atoms, thus acquiring the necessary delocalization to ensure the metallic character of the system. Consequently, the Tr_{11} cluster in the A_8Tr_{11} phases should be formally described as Tr_{11}^{8-}.

Even though this conclusion is clear, we note that it raises a serious question. The present first-principles and previous extended Hückel studies[2,4,9,11] lead to the same conclusion concerning the electronic requirements for stability of the Tr_{11} cluster. However, according to the extended Hückel studies, the lowest empty level of the Tr_{11}^{7-} unit is a degenerate set of e-type orbitals so that, if the extra electron fills them, a Jahn−Teller distortion breaking the D_3 (or D_{3h}) symmetry of the cluster should be observed. To avoid this, the formulation $Tr_{11}^{7-}(e^-)$ was postulated in these studies. However, our first-principles calculations show that this description is not appropriate. Thus, we must consider in more detail the nature of the level accommodating the extra electron. We first carried out calculations for the Tr_{11}^{7-}

(18) Perdew, J. P.; Burke, K.; Ernzerhof, M. *Phys. Rev. Lett.* **1996**, *77*, 3865.
(19) Troullier, N.; Martins, J. L. *Phys. Rev. B* **1991**, *43*, 1993.
(20) Kleinman, L.; Bylander, D. M. *Phys. Rev. Lett.* **1982**, *48*, 1425.
(21) Anglada, E.; Soler, J. M.; Junquera, J.; Artacho, E. *Phys. Rev. B* **2002**, *66*, 205101.
(22) Artacho, E.; Sánchez-Portal, D.; Ordejón, P.; García, A.; Soler, J. M. *Phys. Status Solidi B* **1999**, *215*, 809.
(23) Monkhorst, H. J.; Park, J. D. *Phys. Rev. B* **1976**, *13*, 5188.

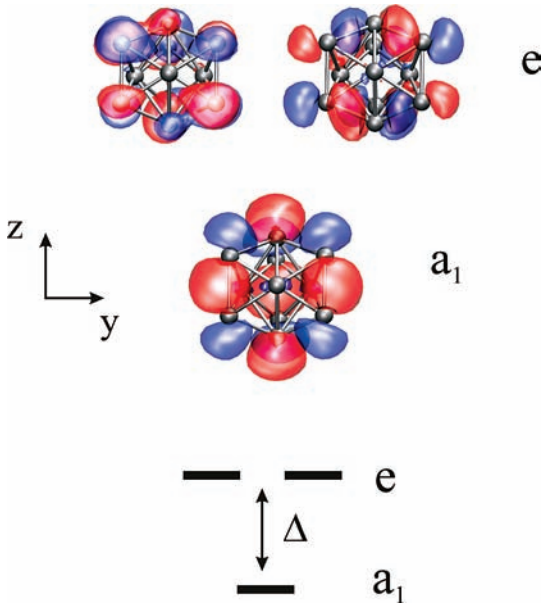

Figure 3. Nature of the lowest empty levels of the Tr_{11}^{7-} cluster.

Table 2. Calculated Energy Gaps [a] between the a_1- and e-Type Empty Orbitals for the Tr_{11}^{7-} Clusters of Different A_8Tr_{11} Phases

Cs_8Tl_{11}	Rb_8Tl_{11}	K_8Tl_{11}	Rb_8In_{11}	K_8In_{11}	Cs_8Ga_{11}	$Cs_8Ga_{11}Cl$
0.56	0.54	0.56	0.38	0.37	0.27	0.27

[a] In eV; see Δ in Figure 3.

clusters as found in the Cs_8Tl_{11}, K_8In_{11}, Cs_8Ga_{11}, $Cs_8Ga_{11}Cl$, Rn_8In_{11}, K_8Tl_{11}, and Rb_8Tl_{11} phases.[24] In all cases we found that the lowest unoccupied orbital is a non degenerate a_1-type orbital and the e-type degenerate set is higher in energy (see Figure 3). The calculated energy gaps between the a_1- and e-type orbitals are reported in Table 2. The gaps are essentially independent of the slight distortions induced in the solid by the rest of atoms around the clusters and decrease from Tl to Ga. Exactly the same trend is obtained when the calculations are carried out for the Tr_{11}^{8-} clusters. The lowest lying non degenerate a_1-type orbital (see Figure 3) is essentially built from $6p_z$ orbitals of the Tr1 and Tr3 atoms in such a way that it leads to antibonding Tr1−Tr3 interactions but keeps bonding Tr1−Tr1 interactions. This orbital is symmetric with respect to the mirror plane (only approximate for the slightly distorted D_3 clusters) cutting the three Tr1−Tr1 bonds. In contrast, the two higher lying e-type orbitals are antisymmetric with respect to this plane and are built from the Tr1 and Tr3 $6p_x$ and $6p_y$ orbitals, respectively. We note that although the contribution of the Tr2 orbitals is small for both types of orbitals (and hence the absence of contributions in the representations of Figure 3) it is is noticeably larger for the e-type orbitals.

To understand why the a_1 orbital is the lowest empty level in these Tr_{11}^{7-} clusters it is useful to look at the Mulliken overlap populations[25] associated with it for each type of bond of the cluster. The calculated overlap populations for the

(24) The calculations are carried out using the same periodic code as for the real A_8Tr_{11} solids using a Tr_{11}^{n-} repeat unit in a large box so as to effectively isolate the different clusters surrounded by a uniformly distributed $n+$ charge. The use of this uniform charge simply induces a rigid shift of all the levels while keeping the neutrality of the system.

(25) Mulliken, R. S. *J. Chem. Phys.* **1955**, *23*(1833), 2343.

Table 3. Calculated Tr−Tr Mulliken Overlap Populations for the Isolated Tr_{11}^{7-} and Tr_{11}^{8-} Clusters as well as the Tr_{11} Clusters in the Complete Solid Structure for Cs_8Tl_{11}, K_8In_{11}, and Cs_8Ga_{11} [a]

	Cs_8Tl_{11}			K_8In_{11}			Cs_8Ga_{11}		
bond	Tl_{11}^{7-}	Tl_{11}^{8-}	Cs_8Tl_{11}	In_{11}^{7-}	In_{11}^{8-}	K_8In_{11}	Ga_{11}^{7-}	Ga_{11}^{8-}	Cs_8Ga_{11}
a	0.127	0.159	0.118	0.167	0.197	0.117	0.165	0.197	0.130
b	0.171	0.155	0.128	0.205	0.188	0.139	0.229	0.197	0.192
c	0.163	0.162	0.133	0.195	0.193	0.140	0.201	0.197	0.165
d	0.144	0.141	0.117	0.167	0.162	0.122	0.186	0.179	0.154
e	0.073	0.073	0.062	0.086	0.085	0.066	0.075	0.072	0.062

[a] See Figure 1b for the labeling of the different Tr−Tr bonds.

Tr−Tr bonds in the isolated Tr_{11}^{7-} and Tr_{11}^{8-} clusters as well as in the A_8Tr_{11} solids are reported in Table 3 for Cs_8Tl_{11}, K_8In_{11}, and Cs_8Ga_{11}. Using the values in Table 3 and taking into account the number of bonds of each type it is easy to find that the total overlap population change due to the occupation of the a_1 orbital is −0.024 for Cs_8Tl_{11}, −0.060 for K_8In_{11}, and −0.180 for Cs_8Ga_{11}. These values are associated with weak antibonding interactions since they are only 17.6%, 36.7%, and 104.7% of the average overlap population of a *single* Tr−Tr bond of the cluster. Thus, the antibonding character introduced in the whole cluster as a result of the occupation of the a_1 orbital is smaller or equal to the bonding character associated with only one of the 27 Tr−Tr bonding interactions of the cluster. It is clear from the values of Table 3 that the antibonding character of this orbital results mostly from the balance between the three bonding Tr1−Tr1 interactions (0.096 for Cs_8Tl_{11}) and the six antibonding Tr1−Tr3 interactions (−0.090 for Cs_8Tl_{11}). The total antibonding character thus coincides approximately with the contribution of the weak (but there are as many as 12 per cluster) Tr1−Tr2 interactions (−0.024 for Cs_8Tl_{11}). In addition, the interaction of the Tr1 and Tr3 atoms with the high lying cesium orbitals may provide an additional source of stabilization as attested by the many slightly positive cluster−cesium overlap populations (but see below). These results suggest that occupation of the a_1 cluster orbital does not represent a strong penalty for the stability of the cluster units. We have tried to understand the reason for the difference in the first-principles and extended Hückel results by looking at differences in the orbital character. We found that in the extended Hückel a_1-type orbital, the $6p_z$ individual contributions of the Tr1 atoms are strongly hybridized with $6p_x$ and $6p_y$ so that one of the lobes points better toward the capping Tr3 atoms, increasing the antibonding character, and the other lobe points outside the Tr1−Tr1 bond, strongly decreasing the bonding character. As a result, in the extended Hückel calculations the a_1 orbital is considerably raised in energy above the e pair.

Now we must turn to the solid to see if this simple bonding picture is modified because of the spread of the cluster orbitals into bands. An analysis of the DOS in the region of interest is shown in Figure 4. We report in Figure 4a the total DOS and cesium local DOS. The thallium contribution clearly dominates in the region around the Fermi level (~80%). The contributions of the three different types of Tl atoms are reported in Figure 4b. The ratio between the Tl1/Tl3/Tl2 contributions around the Fermi level is 11.1:2.2:1 whereas the ratio between the number of atoms is 3:1:1.5 so that it is clear that the extra electron fills levels which are mainly Tl1 and Tl3 in character and only weakly Tl2. The two

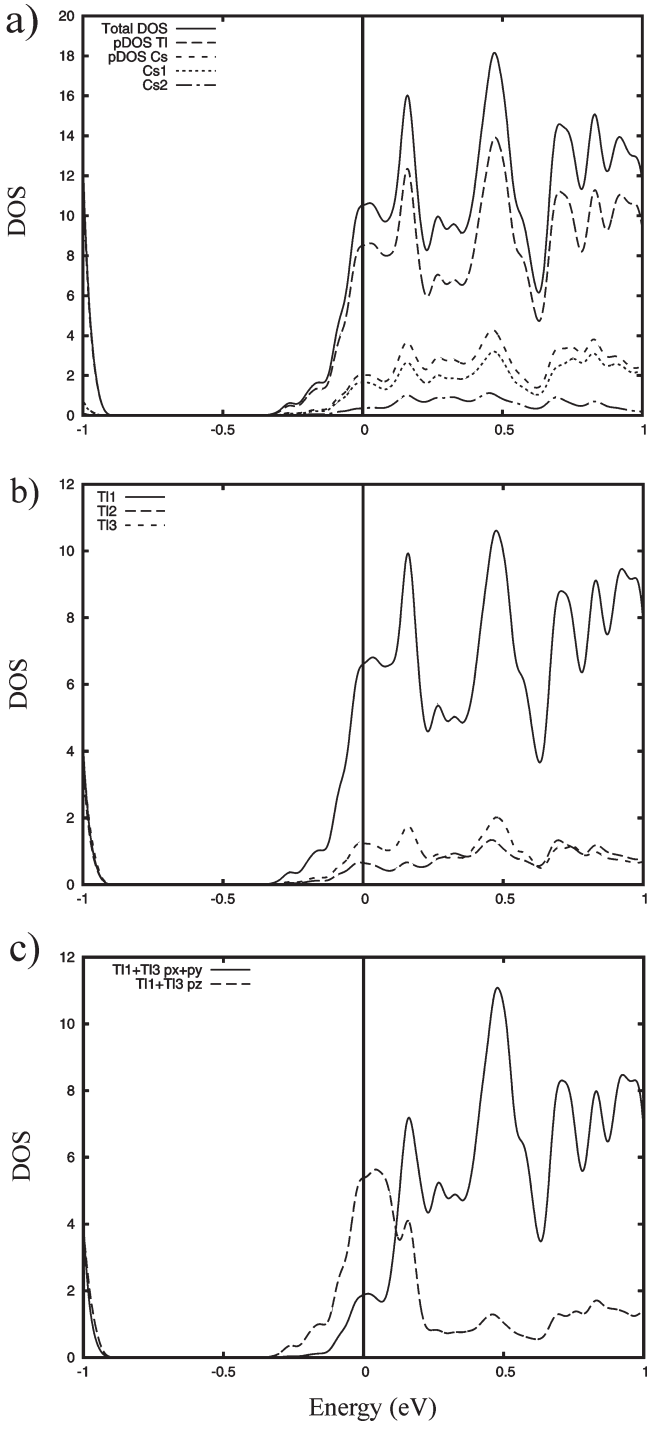

Figure 4. (a) Calculated DOS in the region around the Fermi level for Cs_8Tl_{11} including the local contributions for all the cluster atoms (Tl) as well as those of the Cs1 and Cs2 atoms; (b) local DOS associated with the three types of Tl atoms; and (c) local DOS associated with the $6p_z$ and $(6p_x + 6p_y)$ orbitals of the Tl1 and Tl3 atoms.

cesium contributions (Cs1 and Cs2) are reported in Figure 4a. The ratio between the Cs1/Cs2 contributions is 4.5:1 whereas the ratio between the numbers of atoms is 2:1. Consequently, the contribution from the alkali-metal atoms in the double layers (Cs1) dominates over the contribution of the alkali-metal atoms in the voids of the cluster layers. These two observations suggest that in the solid it is also the a_1-type orbital which accommodates the extra electron. Since in the following this will prove to be a key feature, we should examine this question in more detail at this point. There is a simple way to distinguish between the contribution of the a_1-type and e-type cluster orbitals to the DOS. As can be seen in Figure 3, the main components of the two orbitals are found in the Tl1 and Tl3 atoms with the important difference that whereas the first (a_1) is mainly built from the $6p_z$ atomic orbitals, the latter (e) are mainly built from the $6p_x$ and $6p_y$ orbitals. Thus, projecting the DOS total contribution of the Tl1 and Tl3 $6p_z$ local contributions and the Tl1 and Tl3 $(6p_x + 6p_y)$ local contributions is an easy way to detect the participation of the cluster a_1- and e-type orbitals in the DOS curves. Taking into account that the first is associated with just one cluster orbital, whereas the second is associated with two of them, the results in Figure 4c very clearly confirm that in Cs_8Tl_{11} the extra electron fills states originating from the cluster a_1-type orbital.

What can be said concerning the cluster−alkali-metal interactions in the solid? The Cs contributions to the filled levels of Figure 2, the decrease in the cluster Tr−Tr overlap populations when comparing the isolated Tr_{11}^{8-} cluster and the solid, as well as the calculated charges for the cations, +0.59 (Cs1) and +0.60 (Cs2), they all suggest an important mixing of the alkali-metal and cluster orbitals. The calculated charges for the K_8In_{11} phase, +0.41 (K1) and +0.46 (K2), are for instance notably smaller than those calculated with the same computational settings for a typical ionic salt of potassium like KF (+0.64). Even bearing in mind the possible shortcomings of a Mulliken population analysis, these results make clear that there is an important contribution of the cesium atoms to the covalent bonding in this phase. Taking into account all Tl−Cs distances below 5.0 Å, every Tl1 is implicated in six interactions, every Tl2 in four, and every Tl3 in six. We have evaluated all these overlap populations and found a very substantial positive cluster−alkali-metal overlap population (1.440 per cluster). A fraction of 66.6% of the total A−Tr overlap population per cluster is associated with the Tl1 atoms, 17.1% with the Tl2 atoms, and 16.2% with the Tl3 atoms. Taking into account the different number of atoms of each type in a single cluster, this means that every Tl1 is associated with 11.1% of the total overlap population, every Tl2 with 5%, and every Tl3 with 8.1%. With small variations we have found similar results for the other phases.[26] Thus, although all cluster atoms contribute to the cluster−alkali-metal bonding, the Tl1 atoms slightly dominate. Every Cs1 is associated with 12.4% of the cluster−alkali-metal overlap population and every Cs2 is associated with 12.7%. Consequently, although the interactions of the cluster with the double layers of alkali-metal atoms are a little bit stronger, the cation−cluster interaction is quite isotropic with a significant covalent character.

The relative weight of the cluster−alkali-metal and Tr−Tr bonding/antibonding contributions to bonding in the Cs_8Tl_{11} phase and the reason for the availability of the a_1 cluster orbital to hold the extra electron can not be conveniently discussed in terms of the Mulliken overlap populations (and their solid state counterpart the Crystal Orbital Overlap Populations, COOP[27]), as we did for the isolated cluster,

(26) Note that in addition to formally changing the cluster charge, the presence of halides in the network of the $A_8Tr_{11}X$ phases substantially perturbs the alkali-metal subnetwork (for instance a shrinkage of the *c* parameter is induced) as well as the alkali-metal-cluster bonding and thus, in that indirect way, also influences the intracluster bonding.

(27) Hughbanks, T.; Hoffmann, R. *J. Am. Chem. Soc.* **1983**, *105*, 3528.

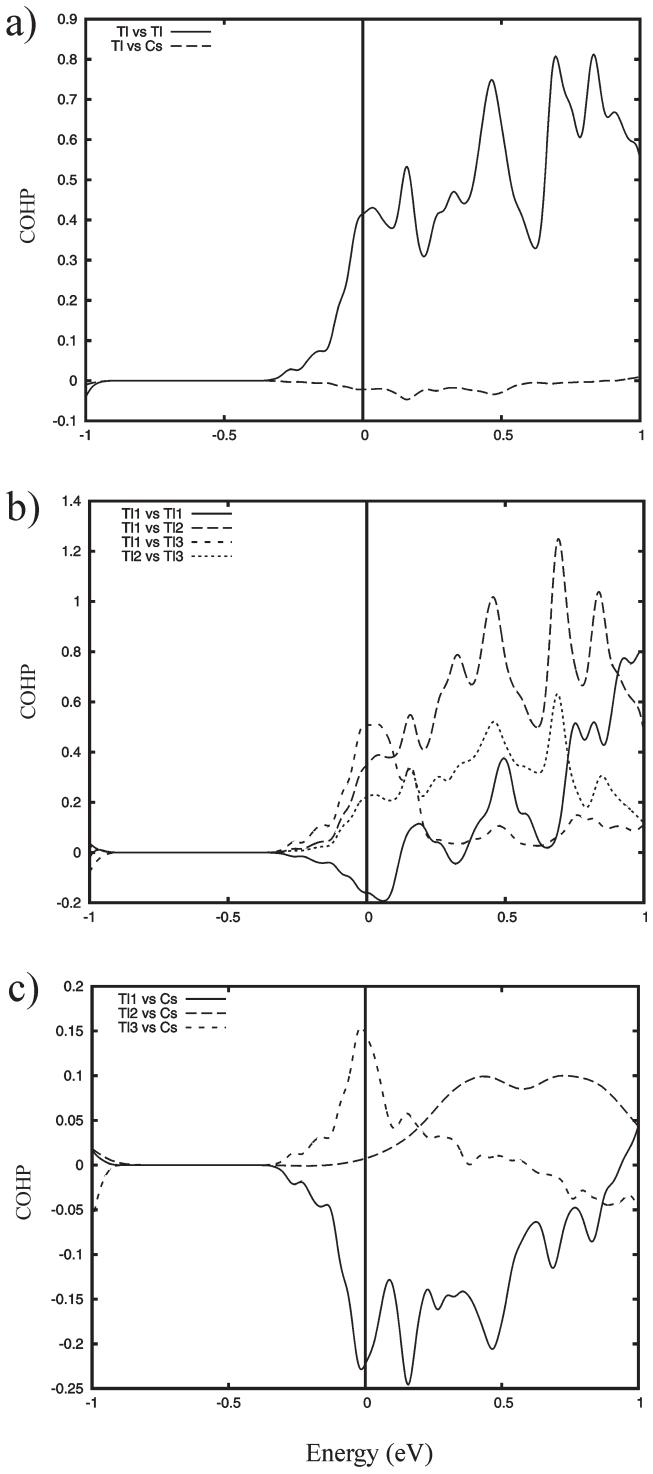

Figure 5. Calculated COHP curves for Cs_8Tl_{11}: (a) total Tl−Tl cluster bonding and total cluster−Cs bonding; (b) total Tl1−Tl1, Tll−Tl2, Tl2−Tl3, and Tl1−Tl3 cluster bonding; and (c) total Tl1−Cs, Tl2−Cs, and Tl3−Cs bonding. Note the different scales for the COHPs.

because it is well-known that overlap populations associated with different pairs of atoms are not comparable (in addition to well-known problems when they implicate relatively different pairs of atoms). In these circumstances, a better adapted tool are the so-called Crystal Orbital Hamilton Populations (COHP)[28−30] curves, which are similar in spirit to the COOP curves. Essentially, in a COHP analysis it is the energy instead of the number of electrons what is partitioned into local contributions. In other words, the COHP curves indicate the contribution of an atom pair to the Kohn−Sham energy of the levels in a given energy region. Although the Kohn−Sham energy is not really the total energy, the COHP curves are a very useful analytical tool quantitatively measuring bond strengths of different pairs of atoms. Shown in Figure 5a are the calculated COHP curves for the total Tl−Tl and Tl−Cs interactions, whereas in Figures 5b and 5c we report plots to analyze the different contributions to these interactions. Note that bonding/antibonding interactions are associated with negative/positive values in the COHP curves, respectively. The first observation is that the cluster−cesium interactions in the region of the extra electron are very weakly stabilizing compared with the intracluster ones. The reason is that from an energetic viewpoint the stabilizing interactions associated with the Tl1−Cs interactions are almost compensated by antibonding Tl3−Cs interactions (see Figure 5c). The bonding cluster−cesium interactions are strong in the lower-lying filled states below the band gap around −0.4 eV. However, they are remarkably weak in the region filled by the extra electron because of the sign changes associated with the orbitals of Tl1 and Tl3 atoms in the a_1 and e antibonding cluster levels which lead to a partial cancellation of the Tl1−Cs and Tl3−Cs contributions. In summary, the bonding cluster−alkali-metal interactions play only a secondary role in stabilizing the levels filled by the extra electron, and we can concentrate on the intracluster interactions. The COHP curves associated with the different intracluster interactions are shown in Figure 5b. Analysis of these curves for the region filled by the extra electron leads to the same picture developed for the isolated cluster: the bonding Tr1−Tr1 and antibonding Tr1−Tr3 almost compensate, and finally the global curve is given by the contribution of the many weak Tr1−Tr2 interactions and the Tr2−Tr3 interactions. Thus, the spread of levels and interaction with the alkali-metal orbitals does not significantly modify our simple explanation put forward for the isolated cluster.

Now we can turn to the second question raised in the introduction: what makes Cs_8Ga_{11} different from the other A_8Tr_{11} phases? We report in Figure 6 the analysis of the DOS for Cs_8Ga_{11} in its hypothetical metallic state. The main features of the DOS apparently are quite similar to those of Figure 4. The only noticeable differences are a somewhat larger participation of the cesium (33.8% vs 19% around the Fermi level) and Tr2 atoms (the ratio between the Ga1/Ga3/Ga2 contributions around the Fermi level is 7.8:1.6:1). Recalling that we noted a somewhat larger participation of the Tr2 atoms in the e-type cluster orbitals, these small variations seem to reflect changes between the nature of the states filled by the extra electron. The slightly larger participation of the Tr2 atoms leads to a slightly larger interaction with the cesium atoms and suggests that the e-based bands should be broader. At this point we must turn back to Table 2 were the energy differences between the a_1- and e-type orbitals in the isolated clusters are reported: this gap has been reduced by a factor of 2 in Cs_8Ga_{11} with respect to that in Cs_8Tl_{11}. Since this gap is just 0.27 eV it is quite likely that a larger interaction with the alkali-metal atoms may

(28) Dronskowski, R.; Blöchl, P. E. *J. Phys. Chem.* **1993**, *97*, 8617.
(29) Dronskowski, R. *Computational Chemistry of Solid State Materials*; Wiley-VCH: Weinheim, 2005.
(30) Glassey, W. V.; Hoffmann, R. *J. Chem. Phys.* **2000**, *113*, 1698.

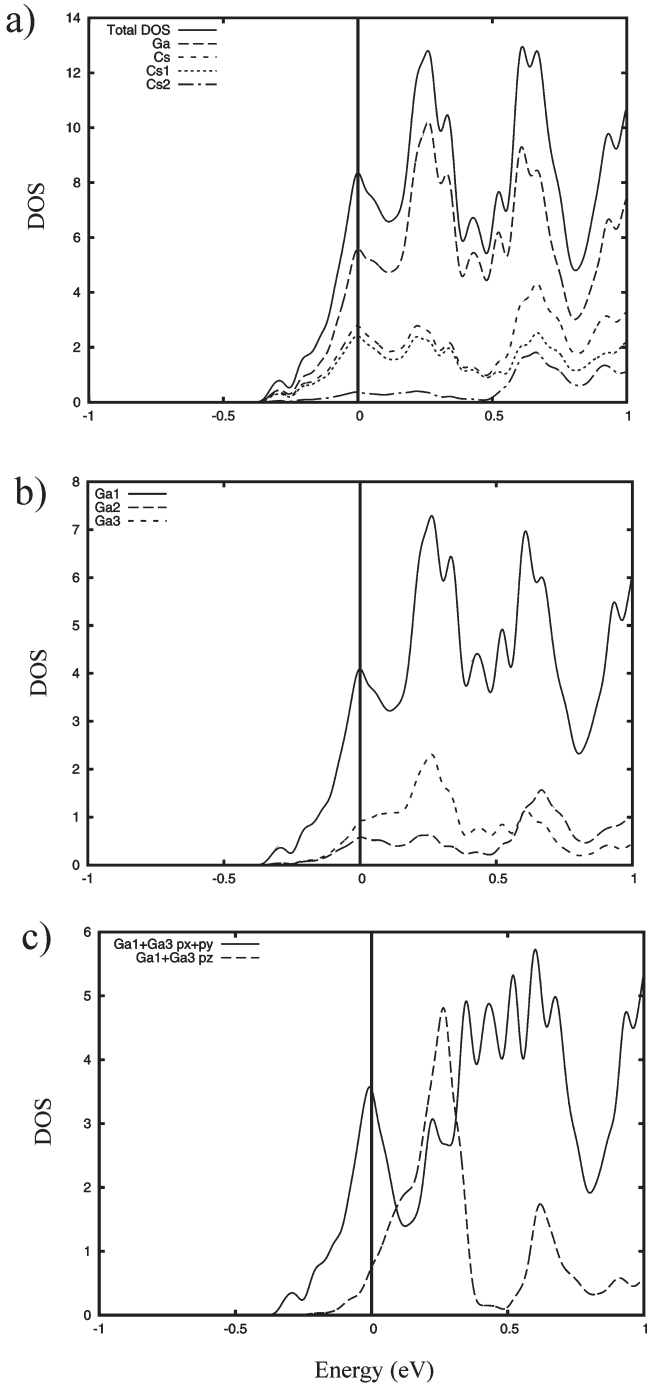

Figure 6. (a) Calculated DOS in the region around the Fermi level for metallic Cs_8Ga_{11} as well as local contributions for all the cluster atoms (Ga), as well as those of the Cs1 and Cs2 atoms; (b) local DOS associated with the three types of Ga atoms; and (c) local DOS associated with the $4p_z$ and $(4p_x + 4p_y)$ orbitals of the Ga1 and Ga3 atoms.

bring an inversion in the nature of the levels filled by the extra electron in the solid. This is confirmed by the results of Figure 6c showing that in Cs_8Ga_{11} the Ga1 and Ga3 $4p_z$ levels are practically empty whereas the Ga1 and Ga3 $(4p_x + 4p_y)$ are the major components of the states filled by the extra electron. Thus, the e-type cluster orbital has become the cluster orbital that is filled with the extra electron for metallic Cs_8Ga_{11}. The same conclusion is reached when the projected DOS of the a_1- and e-type orbitals of an isolated Tr_{11}^{7-} cluster are examined (see Supporting Information, Figures

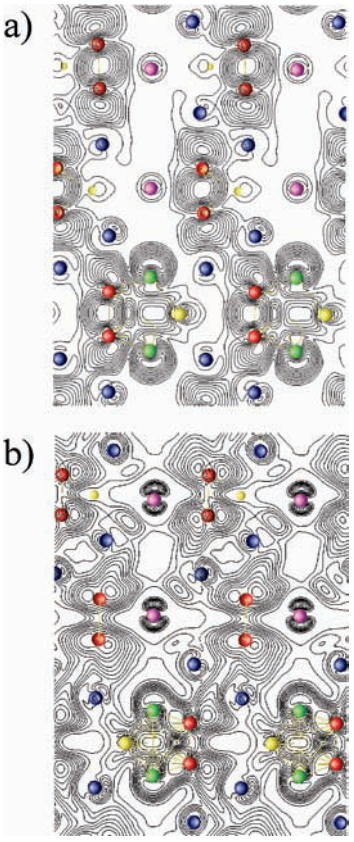

Figure 7. Electron density associated with the levels filled by the extra electron for (a) Cs_8Tl_{11} and (b) metallic Cs_8Ga_{11}, in a plane including one Tr1−Tr1 bond as well as the Tr3 capping atoms of the clusters situated at the bottom of the plot. For simplicity, only half of the plot along the *c*-direction of the hexagonal cell is represented. Note the very different shape in the vicinity of the Tr1−Tr1 cluster bonds indicating accumulation/depletion of electron density for Cs_8Tl_{11} (a)/Cs_8Ga_{11} (b), respectively. Tr1: red, Tr2: yellow, Tr3: green, Cs1: blue and Cs2: purple.

S1 and S2). Let us note that calculations for the diamagnetic semiconductor $Cs_8Ga_{11}Cl$ led to an identical analysis of the DOS except for the fact that (a) the states above the gap around −0.4 eV are now empty, and (b) there are new low-lying filled 3s and 3p Cl peaks.

An even more direct proof for the change in the nature of the highest filled cluster orbital between Cs_8Tl_{11} and Cs_8Ga_{11} is provided by the plots in Figure 7. There we represent the electron density for the states found between the gap around −0.4 eV and the Fermi level (i.e., the levels filled by the extra electron) for a plane including one Tr1−Tr1 bond as well as the Tr3 capping atoms of the lower clusters (for simplicity, we only represent half of the plot along the *c*-direction of the hexagonal cell). Looking at the pair of clusters at the bottom of the plot it is immediately clear that there is an accumulation of electronic density in the region of the Tr1−Tr1 bond for Cs_8Tl_{11} (Figure 7a) whereas there is a decrease for Cs_8Ga_{11} (Figure 7b), nicely reflecting the Tr1−Tr1 bonding character of the a_1 orbital filled for the former and the Tr1−Tr1 antibonding character of the e orbitals filled for the latter. The calculated gaps between the a_1 and e levels of Table 2 suggest that the tendency to fill the e-type cluster level progressively increases from Tl to In and Ga. Our calculations for the intermediate K_8In_{11} phase show that this is indeed the case, although it is only for Cs_8Ga_{11} that the inversion has occurred.

The e vs a_1 cluster orbital occupation by the extra electron is an essential difference which we believe is at the heart of the different conductivity behavior of the Cs_8Ga_{11} phase. By populating the cluster e-type level, the phase is susceptible to a structural instability of the Jahn−Teller type, destroying the 3-fold symmetry axis of the clusters, which would affect the whole structure through the many cluster−alkali-metal bonding interactions. However, the system has a way to avoid such instability without undergoing any structural change just by restoring the "natural" filling of the cluster levels, that is, by filling the a_1 level at the expense of the e level. It simply needs to reduce the interactions of the alkali-metal atoms with the e- and a_1-type cluster levels since in that way, the cluster levels will not substantially spread in the solid and will recover the a_1 below e level ordering of the isolated cluster, thus avoiding in this way the structural instability by localizing the extra electron on the cluster. The price to be paid for this localization is that the electronic conduction must now be activated. Note that according to this suggestion in both the Cs_8Tl_{11} and the Cs_8Ga_{11} phases the a_1 cluster orbital is filled with one electron, although in the former it delocalizes whereas in the latter it remains localized in the cluster. Consequently, the comparison between Cs_8Tl_{11} to Cs_8Ga_{11} can be seen as a kind of Mott localization process induced by the need to avoid a structural instability of the metallic phase in the latter. It is interesting to note that this way to avoid the structural instability by localizing the electrons related with the metallic behavior is, in some way, reminiscent of the explanation for the origin of ferromagnetism in bcc-Fe put forward by Dronskowski et al.[31] There, by undergoing a spin polarization process decreasing the population of Fe−Fe antibonding levels near the Fermi level of the metallic state, the system may be stabilized without undergoing any structural change. Thus, in both cases there is a purely electronic mechanism avoiding the structural instability which leaves the crystal structure unaltered but that has strong consequences for the physical properties.

(31) Landrum, G. A.; Dronskowski, R. *Angew. Chem., Int. Ed.* **1999**, *38*, 1389.

Concluding Remarks

As perceptively noted by Corbett et al.,[2,4,8,10] the need for extra alkali-metal atoms in phases like A_8Tr_{11} must result from packing requirements. The beauty of the A_8Tr_{11} phases lies in the fact that by adopting the peculiar shape of the clusters that they do, the electron deficiency with respect to Wade's rules can be accommodated while, at the same time, the extra electron with respect to its optimum electron count does not introduce severe antibonding interactions. Although this extra electron could induce some structural instability depending on the nature of the Tr atom, the system has at its disposal a purely electronic mechanism to avoid it while changing the nature of the electronic conductivity. There is certainly a very subtle interplay of packing and bonding requirements at work behind the structure and transport properties of these quite unique phases.

Acknowledgment. We thank Professor J. D. Corbett for bringing this problem to our attention. This work was supported by DGES-Spain (Projects FIS2006-12117-C04-01, CSD2007-00041 and CTQ2008-06670-C02-02/BQU), CSIC (PIE 200660I129) and Generalitat de Catalunya (Project 2005 SGR 00036). Part of the computations described in this work were carried out using the facilities of CESCA and CESGA. AG was supported by the ESF under the EUROCORES Programme EuroMinScI (contracts ERASCT-2003-980409 of the European Commission, DG Research, FP6, and CGL2005-25095-E of the Spanish MEC).

Supporting Information Available: Additional information as noted in the text. This material is available free of charge via the Internet at http://pubs.acs.org.